Rock and Soil Mechanics

Volume 41 | Issue 2 Article 10

9-27-2020

Seismic response of pile-soil-structure in coral sand foundation under different earthquake intensities

Qi WU
Key Laboratory of New Technology for Construction of Cities in Mountain Area, Chongqing University, Chongqing 400045, China

Xuan-ming DING
Key Laboratory of New Technology for Construction of Cities in Mountain Area, Chongqing University, Chongqing 400045, China, dxmhhu@163.com

Zhi-xiong CHEN
Key Laboratory of New Technology for Construction of Cities in Mountain Area, Chongqing University, Chongqing 400045, China

Yu-min CHEN
College of Civil and Transportation Engineering, Hohai University, Nanjing, Jiangsu 210098, China

See next page for additional authors

Custom Citation

WU Qi, DING Xuan-ming, CHEN Zhi-xiong, CHEN Yu-min, PENG Yu, . Seismic response of pile-soil-structure in coral sand foundation under different earthquake intensities[J]. Rock and Soil Mechanics, 2020, 41(2): 571-580.

Seismic response of pile-soil-structure in coral sand foundation under different earthquake intensities

Authors

Qi WU, Xuan-ming DING, Zhi-xiong CHEN, Yu-min CHEN, and Yu PENG

Rock and Soil Mechanics 2020 41(2): 571−580 ISSN 1000−7598
https: //doi.org/10.16285/j.rsm.2019.5122 rocksoilmech.researchcommons.org/journal

Seismic response of pile-soil-structure in coral sand foundation under different earthquake intensities

WU Qi[1, 2], DING Xuan-ming[1, 2], CHEN Zhi-xiong[1, 2], CHEN Yu-min[3], PENG Yu[1, 2]

1. College of Civil Engineering, Chongqing University, Chongqing 400045, China
2. Key Laboratory of New Technology for Construction of Cities in Mountain Area, Chongqing University, Chongqing 400045, China
3. College of Civil and Transportation Engineering, Hohai University, Nanjing, Jiangsu 210098, China

Abstract: The dynamic field response to earthquake in the coral sand is affected by its special engineering properties. In order to reveal the seismic response characteristics of the pile-soil-superstructure in the coral sand site, the shaking table tests of pile groups with three-storey frame structure in coral sand under different earthquake intensities are carried out. The dynamic responses to soil and structure are analyzed and compared with those in the liquefied quartz sand of Fujian. The results show that the excess pore water pressure ratios in both coral and quartz sands are far less than 1 under 0.1g seismic intensity, demonstrating that no liquefaction occurs in both sites. However, both coral and quartz sands are liquefied under 0.2g seismic intensity, and the liquefaction degree of coral sand is less than that of quartz sand. Compared with the quartz sand site, the coral sand site still has some shear strength and stiffness after the liquefaction. The settlement, horizontal displacement and column bending moment of coral sand site under 0.1g and 0.2g seismic intensities are smaller than those of quartz sand site. The position of peak bending moment of pile foundation under different seismic intensities is not the same.

Keywords: coral sand; shaking table test; pile group; dynamic response; excess pore water pressure

1 Introduction

Due to the particular marine biogenesis, the coral sand often shows the physical properties of irregular shaped particles, easily breaks, porous etc., making its mechanical property (e.g., strength, deformation, infiltration etc.) different from that of the terrestrial sand[1−5]. The strategy of ocean strong power makes the implementation of a series of hydraulic reclamation engineering in the coral islands and reefs. All kinds of buildings are constructed in the islands, making the safety of anti-seismic very important. The previous seismic events in the coral islands and reefs show that the liquefaction of coral sand is the main reason for the destruction of all kinds of buildings. To reveal the particular liquefaction characteristics of the coral sand, the dynamic triaxial experiments are often applied to study the evolution of strength, deformation and pore pressure of the saturated coral sand under the dynamic load. It demonstrates that the liquefaction of the coral sand is more difficult than that of the terrestrial sand[6−10].These studies mainly aim at the liquefaction characteristics of coral sand. However, all kinds of buildings exist in the foundation of coral sand. The interaction between the foundation and structure under the impacts of earthquake plays a significant role in controlling the dynamic response of the foundation and structure. As one of the common foundation styles, the pile foundation is widely applied in the construction of coral islands. The mechanics properties under the static load of the pile foundation in the coral sand are widely studied at home and abroad[11−14]. However, when the pile foundation exists, studies on the mechanics characteristics of all kinds of buildings under the dynamic load are seldom.

The shaking table test is an important method to study the dynamic responses of all kinds of buildings and foundation under the earthquake conditions. Chau et al.[15] carried out the shaking table test to study the impacts of Elcentro earthquake in 1940 on the single-layer steel structure model supported by four point bearing piles. It demonstrates that the destruction of the pile is maybe caused by the vibratory impulse of the pile near the driving hood and the lateral compressed soil. Rasouli et al.[16] investigated the effect of reducing the settlement of low-layered building through adding different kinds of sheet piles in the shaking table tests. Taking the Shengli bridge of the Tangshan earthquake as the prototype, Tang et al.[17] analyzed the dynamic response of the pile-soil-bridge structure to earthquake, and the failure forms of the pile foundation of the bridge. The dynamic response characteristics of the pile-soil-structure in the terrestrial sand field were also widely studied[18−21].

In this paper, we apply the shaking table tests to study the dynamic response of the coral sand foundation and the

Received: 22 January 2019 Revised: 21 May 2019
This work was supported by the National Natural Science Foundation of China (51622803, 51878103, 41831282).
First author: WU Qi, male, born in 1992, PhD candidate, specializing in the earthquake liquefaction. E-mail: wq_cqu@l63.com.
Corresponding author: DING Xuan-ming, male, born in 1980, PhD, Professor, Research interests: soil mechanics, ground foundation engineering, soil dynamics, engineering vibration and environmental geotechnics. E-mail: dxmhhu@163.com

buildings affected by the dynamic interaction of the pile-soil-structure. Different dynamic response characteristics of the field under different earthquake intensities were studied and compared with that of the Fujian sand field. By comparing the difference and similarities of the dynamic characteristics of the foundation and structure in two different sand fields, it can provide reference for the anti-seismic design of the pile foundation engineering of the coral islands and reefs in the South China Sea.

2 Experimental setup

The shaking table for simulating earthquakes, with a dimension of 1.2 m×1.2 m, located at the civil engineering experimental center of Chongqing University, is applied in the tests. The two-way vibration of horizontal and vertical directions can be realized by using the hydraulic loading. The shaking table has a maximum load of 1 ton, a maximum horizontal displacement of 100 mm, and a maximum acceleration speed of 2.0*g*. The foundation soil is installed in the rigid model box. The dynamic signal collection system of 96 channels is used to receive the signal data from all kinds of sensors.

2.1 Design of similarity ratio

Based on the Bockingham π principle and related research background[22–24], we use the geometrical dimension L, elastic modulus E, and equivalent density ρ as the basic physical parameters. According to the load capacity and the dimension of model, the similitude ratio of the geometry in the test is 1:40. The similitude ratio of the elastic modulus E_r is the elastic modulus ratio of the material made of model building and the concrete material of prototype buildings. The equivalent density ratio ρ_r is calculated by the Eq.(1) when the similitude ratio of predetermined acceleration a_r is 1. The similarity relationship and similarity ratio of other physical parameters is shown in the Table 1.

$$a_r = \frac{E_r}{\rho_r L_r} \tag{1}$$

Table 1 Similitude ratios of physical parameters used in shaking table tests

Physical parameters	Physical symbol	Similitude relationship	Similitude ratio
Geometrical dimension	L	L_r	1:40
Equivalent density	ρ	ρ_r	6:1
Elastic modulus	E	E_r	3:20
Acceleration	a	$a_r = E_r \rho_r^{-1} L_r^{-1}$	1
Time	t	$t_r = E_r^{-0.5} \rho_r^{0.5} L_r$	0.158
Frequency	ω	$\omega_r = t_r^{-1}$	6.325
Stress	σ	$\sigma_r = E_r$	3:20
Linear displacement	S	$S_r = L_r$	1:40

2.2 The preparation of model foundation and structures

The sand rain method is applied to prepare the model foundation. The model case is divided into two parts along the direction of vibration. One part is used to prepare the coral sand model foundation, the other part is used to make the Fujian sand model foundation. The cystosepiment is placed between these two models to avoid the mixing. Most of the energy exists in the form of wave along the vibration direction. The response perpendicular to the vibration direction is small. Therefore, the wave damping effect of the separator plays a minor role in the experimental results. The coral sand used in the experiments is obtained from an island and reef of South China Sea. The average grain diameter d_{50} is 0.48 mm, the uniformity coefficient C_u is 2.67, the relative density of grain G_s is 2.80, the maximum dry density $\rho_{d,max}$ is 1.48 g/cm^3, and the minimum dry density $\rho_{d,min}$ is 1.15 g/cm^3. The Fujian sand used in the experiments is the standard Fujian sand. The average grain diameter d_{50} is 0.60 mm, the uniformity coefficient C_u is 4.50, the relative density of grain G_s is 2.63, the maximum dry density $\rho_{d,max}$ is 1.64 g/cm^3, and the minimum dry density $\rho_{d,min}$ is 1.35 g/cm^3. The grain size distribution of two kinds of sand is shown in Fig.1, illustrating that the grading of these two kinds of sand is similar. To make the relative compaction of the coral sand and Fujian sand approximately the same, the drop distance of these two kinds of sand to the water surface should be kept nearly the same in preparation of samples based on Ma et al. [25]. Other impact factors, including the migration rate of the sanding head, flow rate etc., also should be kept consistency. The calibration aluminum box is applied for the sampling analysis during the preparation of the model foundation. This is to ensure the uniformity and the relative compactness of these two kinds of sand models approximately the same. Finally the relative compactness of the field model foundation of these two kinds of sand is about 0.52, while the corresponding dry density of coral sand is 1.30 g/cm^3, and the dry density of Fujian sand is 1.49 g/cm^3. To keep consistency with the practical engineering,

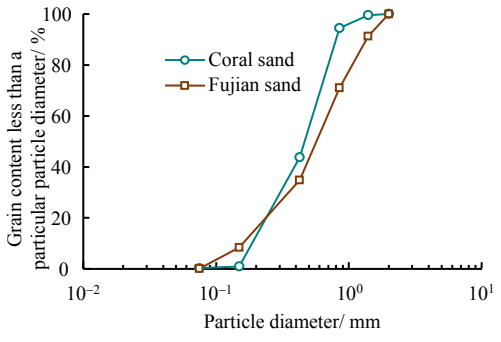

Fig.1 Grain-size distribution curves of coral and Fujian sands

a thickness of 30 mm dry sand layer is covered on the foundation of saturated model. It can be placed 24 hours after preparation of the model foundation.

The prototype of model building is a three layered concrete frame structure in the foundation with four piles. When it is reduced based on similitude ratio, the dimension of model building is so small that the pouring quality of concrete is very difficult to be controlled. Thus the polymethyl methacrylate (PMMA) is used in the production of model. The cross sectional dimension of the model building pillar is 10 mm×10 mm. The PMMA of 5 mm thick is used to separate different layers. The rectangular solids with the dimension of 5 mm× 5 mm×160 mm, made of the PMMA, is installed to simulate the beams under the PMMA. The external rim is parallel with the outer edge of the pile. The side length of the frame structure is 180 mm, the net height of the bottom layer is 100 mm, the net height of the second and third layer is 90 mm. The side length of raft is 220 mm, the thickness is 15 mm. The diameter of model pile is 20 mm, the length is 400 mm. The specific glue used for the PMMA is used to connect different model elements to ensure the perpendicularity of components and integrity of model during the linking process. The undermanual quality model is applied for the upper frame structure and raft. The steel plates, with a dimension of 150 mm×150 mm× 20 mm in the length, width and height, are bonded to each floor of the model building. The mass of each layer is 3.5 kg. The steel plate with a thickness of 6.2 kg and a dimension of 150 mm×150 mm×35.5 mm, is bonded to the raft. The total balance weight of model is 16.7 kg, accounting for 81% of the whole mass. The gravity model is negligible in the pile foundation[26–27].

2.3 The design of working conditions and layout of sensors

Two working conditions of experiments, including the coral sand field and Fujian sand field under different earthquake intensities, are designed and listed in Table 2. The white noise with the intensity of 0.02*g* is input for 20s before and after each vibration. The same layout of sensors is used in these two sand fields, as shown in Fig.2. The laser displacement sensor L1 is fixed on the surface of shaking table through the rigid support and it has a 330 mm distance with the surface of model foundation.

Table 2 Layout of working conditions in experiments

Number of working condition	Relative compaction	Loading waveform	Acceleration amplitude / *g*	Vibration period/ s	Vibration frequency / Hz
1	0.52	Sine wave	0.1	10	5
2	0.52	Sine wave	0.2	10	5

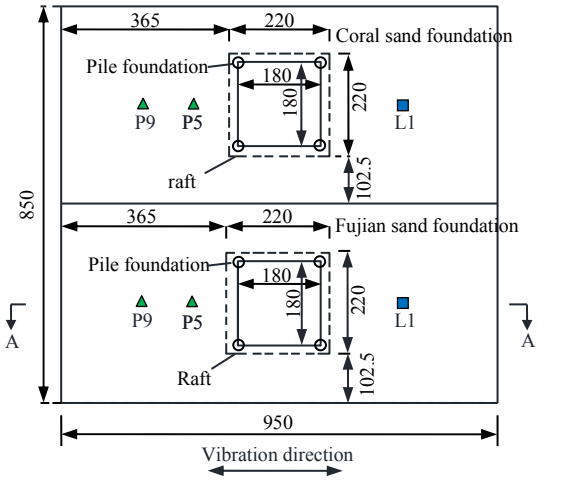

(a) Schematic diagram of layout plan（unit: mm）

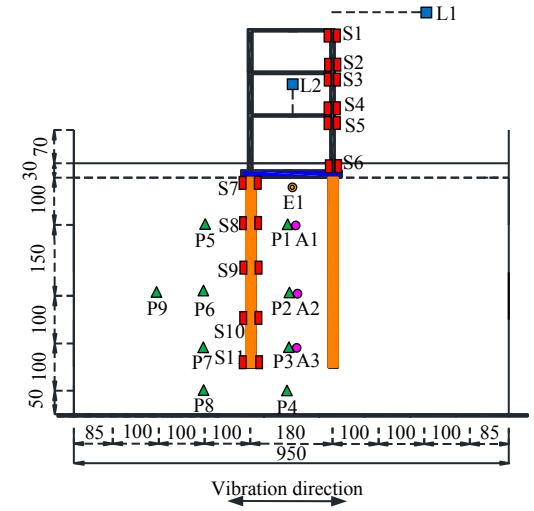

(b) Schematic diagram of sensors plan along the A-A profile（unit: mm）

Fig. 2 Schematic diagram of model layout

3 Macroscopic phenomenon

The field condition before the experiments is shown in Fig. 3(a). In the working condition 1, the field buildings of the coral sand shakes slightly with the input of vibration stimulation. No water discharges from the surface of model foundation. The experimental phenomenon of the Fujian sand field is similar with that of the coral sand. The field condition after the experiments is shown in Fig. 3 (b).

For the working condition 2, the field condition is similar to that of the working condition 1, while the field condition after the experiments is shown in Fig.3(c). During the vibration process, with the input of the vibration stimulation, the shaking degree of buildings on these two kinds of sand fields gradually strengthens. It reaches the maximum around 2 s and then decreases suddenly. The liquefaction of field occurs at this moment. With the input of vibration stimulation, the shaking

degree of buildings gradually strengthens, especially the coral sand field. The water discharges from the surface of model foundation after the 5 s input of vibration stimulation, see Figs. 4(a), (b). The subsidence and leaning of the buildings occur, while the uplift at both sides of the foundation of the buildings appears. After the vibration, the buildings at the two kinds of sand fields lean along the vibration direction, see Fig. 4(c). The dynamic response of the Fujian sand field is much stronger than that of the coral sand field, making a much stronger leaning of the building.

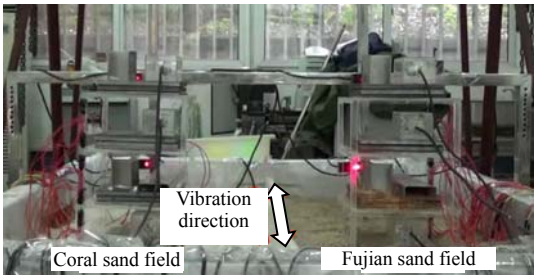

(a) The field condition before the experiments

(b) The field condition after the experiments (a=0.1g)

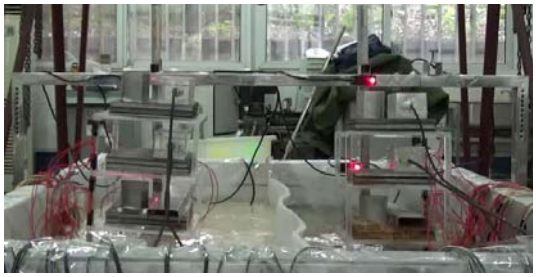

(c)The field condition after the experiments (a=0.2g)

Fig.3 Macro-phenomena at the site before and after test

4 Analysis of foundation soil response

The variation of the excess pore pressure ratio with time at both the coral sand and Fujian sand fields under the building (e.g., P1, P2, P3, P4) is shown in Fig.5. The earth pressure is calculated based on the elastic theory of soil mechanics. The bearing ratio of pile-soil is measured by the earth pressure cell buried under the model raft. In the working condition 1 (0.1g), the evolution of pore pressure in two kinds of model foundation with time differs within 10 s input of vibration stimulation. The excess pore pressure ratio of coral sand field rapidly increases during the period of 2 s. Then it gradually increases till the end of vibration. After the 2 s of rapid growth, the excess pore pressure ratio of Fujian sand field attains the peak value and decreases afterwards. During the rapid increase period of excess pore pressure (0–2 s) , the development of excess pore pressure at the coral sand field is obviously smaller than that of Fujian sand field.

The peak values of excess pore pressure ratio at two different kinds of sand fields are shown in Table 3. The excess pore pressure ratio at each observation point is smaller than 1. No liquefaction is found in the model foundation. The ratio of peak values of excess pore pressure at the coral sand field is about 0.5–0.6 times that of the Fujian sand field. The excess pore pressure ratio of the model foundation in the coral sand gradually decreases with depth. It is highly affected by the stress state, i.e., the excess pore pressure ratio varies inversely with the surrounding pressure and vertical stress. The similar variation rule is suitable for that of the excess pore pressure with depth.

In the working condition 2 (0.2g), after 2 s of rapid growth in the excess pore pressure ratio at two sand fields during the input period of vibration, it varies in a small range. The dissipation rate of excess pore pressure increases after vibration. The peak values of excess pore pressure ratio at two kinds of sand fields are shown in Table 3. Except the P4 at the bottom of model foundation in the coral sand field, the model foundation reaches the liquefaction state because the maximum excess pore pressure ratio basically reaches or more than 0.8[28]. With the increase in the buried depth, the liquefaction of the foundation models at two sand fields gradually weakens. The sand layers with shallow buried depth are more easily to be liquefied and last a much longer period (Fig.5). This is consistent with the general rules of the foundation liquefaction. The excess pore pressure ratio at the coral sand field is about 0.8–0.9 that of the Fujian sand field. Under the same condition, the liquefaction degree of coral sand field is less than that of the Fujian sand field. The coral sand field is more difficult to be liquefied. Compared with the quartz sand, the particle shape of coral sand is more irregular and the conjugation between particles is much stronger. The coral sand is rich in pores, resulting in a slower pore pressure and a much higher anti-liquefaction capacity. Compared with the working condition 1 (0.1g), the excess pore pressure ratio at two sand fields of working condition 2 obviously increases and liquefaction occurs in the foundation. The input intensities of vibration plays a significant role in the liquefaction of foundation. Under the two working conditions,

the excess pore pressure at the same horizontal elevation increases accordingly with the distance to the buildings. A much larger excess pore pressure ratio appears at the location far away from the buildings. The existence of buildings restrains the development of excess pore pressure in the sand fields.

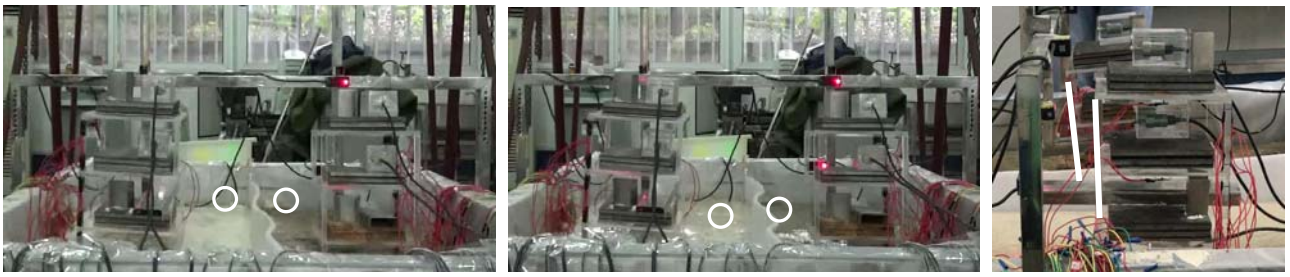

(a) Water emitting from the surroundings of models(t=5 s) (b) Water seeping at the surface (t=7 s) (c) Obvious inclination of buildings (t=10 s)

Fig.4 Macroscopic phenomena at sites during the testing process (a=0.2g)

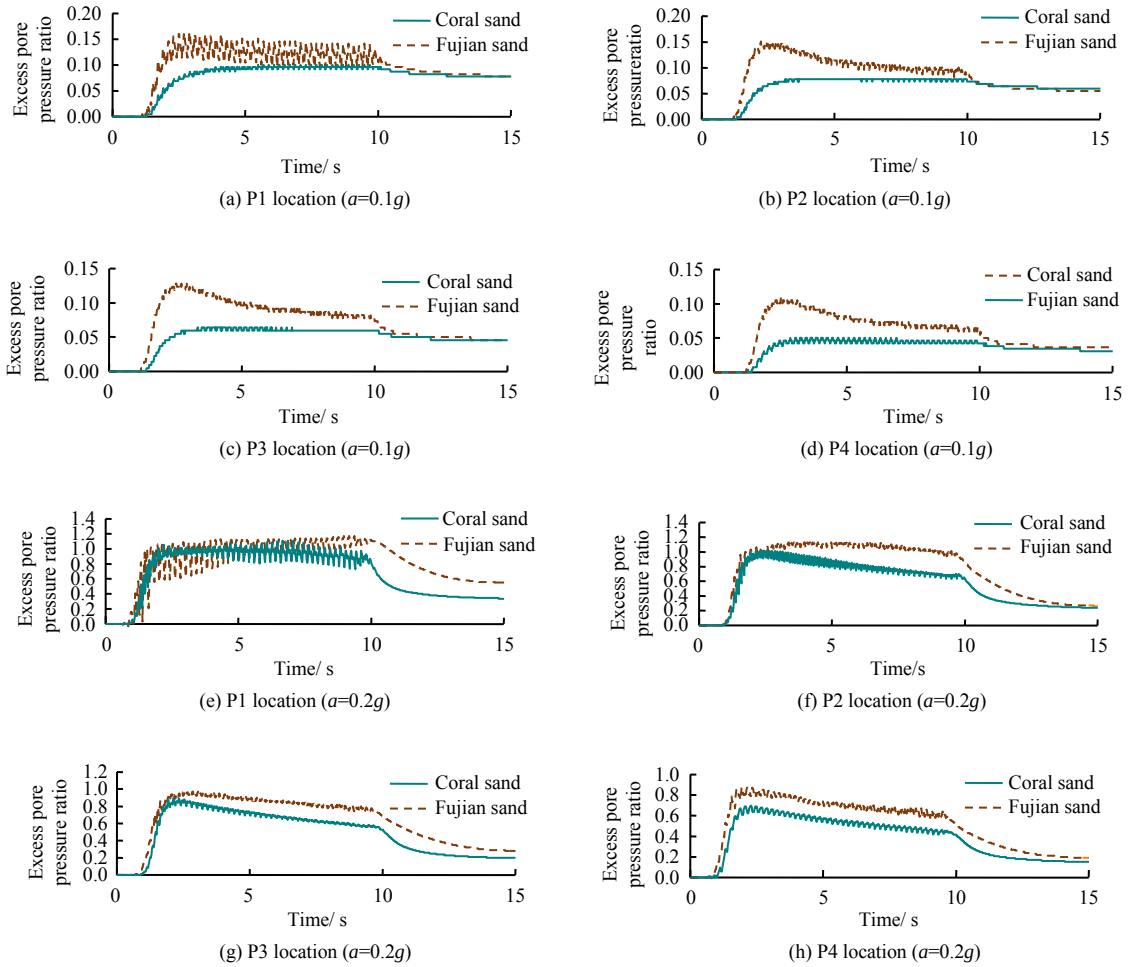

(a) P1 location (a=0.1g) (b) P2 location (a=0.1g)

(c) P3 location (a=0.1g) (d) P4 location (a=0.1g)

(e) P1 location (a=0.2g) (f) P2 location (a=0.2g)

(g) P3 location (a=0.2g) (h) P4 location (a=0.2g)

Fig.5 Time histories of excess pore pressure ratio

Table 3 Comparison of peak values of excess pore pressure ratio

Vibration intensity	Sandy soil types	P1	P2	P3	P4	P5	P6	P7	P8	P9
0.1g	Coral sand	0.10	0.08	0.06	0.05	0.15	0.09	0.07	0.06	—
	Fujian sand	0.16	0.15	0.13	0.11	0.24	0.17	0.14	0.11	0.20
0.2g	Coral sand	1.11	1.02	0.90	0.70	1.40	1.16	0.94	0.74	—
	Fujian sand	1.17	1.14	0.97	0.88	1.60	1.26	1.00	0.81	1.27

The evolution of acceleration with time of the input sine wave is shown in Fig. 6. The time histories of acceleration with time for the coral sand and Fujian sand fields are shown in Figs. 7–9. Under the working condition 1, the acceleration at two sand fields increases rapidly for 1.5 s, followed by slow increases until the end of vibration. The amplification coefficients at different buried depths are shown in Fig. 10. The amplification coefficients of foundation at two different sand fields gradually increase with the elevation and they are larger than 1 for different elevations. The evolution degree of excess pore pressure in the model foundation is small. The soil structure has not changed significantly, and it is still in elastic state as a whole, thus making an amplification effect on the input acceleration of soil. The amplification coefficient of coral sand is smaller than that of the Fujian sand, showing a ratio of 0.98, 0.94 and 0.95 from top to bottom (A1–A3). The stiffness of coral sand field is much larger, which is related with the stronger conjugation of particles in coral sand and the evolution of low pore pressure.

For the working condition 2, the acceleration rates at the two sand fields rapidly increase during 0–1.5 s and it reaches the peak value in about 1.5 s. No liquefaction occurs at the foundation of model at this moment. It still has a certain stiffness and shearing transfer capacity, thus an amplification effect occurs for the input acceleration. During the period of 1.5–10 s, the acceleration rates at the two sand fields weaken, and liquefaction occurs at the model foundation. The non-linear characteristics of the soil body increases, thus its stiffness and shearing transfer capacity weakens. The attenuation of the acceleration rates at two kinds of sand fields is much larger in the soil with a much shallower depth. The acceleration response after the sand liquefaction (>1.5 s) becomes much stronger with buried depth. It is consistent with the general rule of earthquake liquefaction.

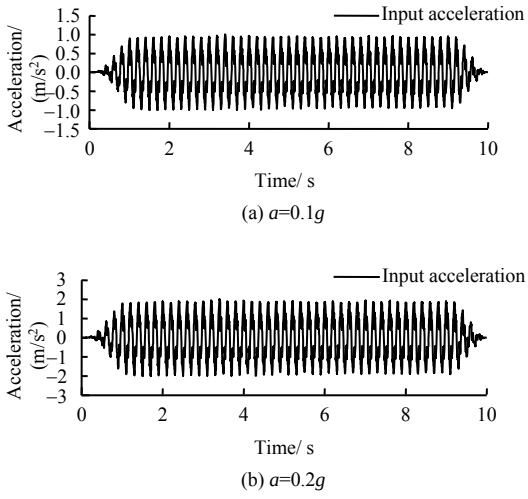

Fig.6 Time histories of input acceleration

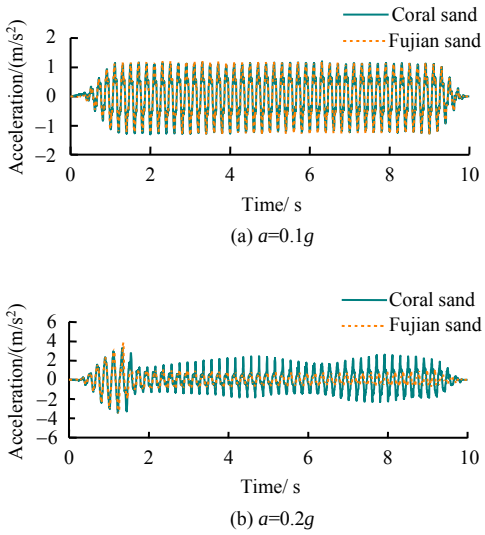

Fig.7 Time histories of acceleration of two sand fields at A1

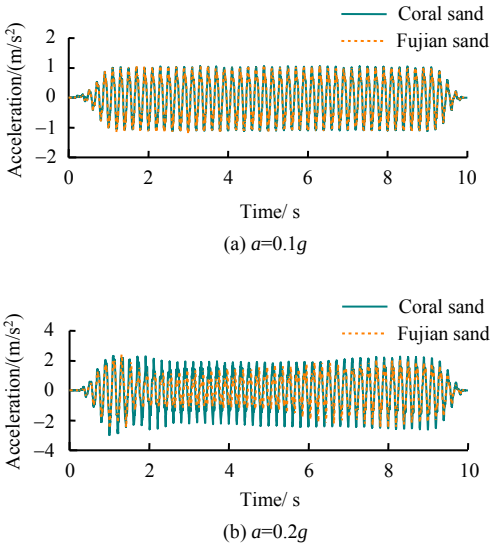

Fig.8 Time histories of acceleration of two sand fields at A2

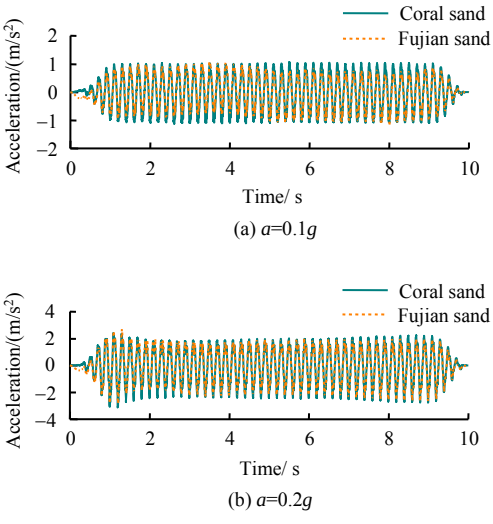

Fig.9 Time histories of acceleration of two sand fields at A3

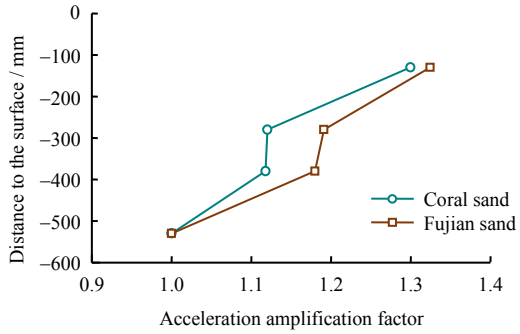

Fig.10 Acceleration amplification factors of two sand fields (a=0.1g)

The acceleration amplification factors after the complete liquefaction of model foundation (after 2 s) are analyzed in Fig.11. It is shown that the acceleration amplification factors of two kinds of sand fields after the liquefaction of model foundation increase with buried depth, which is consistent with the variation trends of excess pore pressure ratio at different buried depths. The acceleration amplification factor at the coral sand field is larger than that of the Fujian sand field, i.e., with the ratio of 2.38, 1.06 and 1.04 at layers A1–A3 from top to bottom. After liquefaction, the shearing transfer capacity of the coral sand field is still stronger than that of the Fujian sand field, and the difference gradually decreases with depth. It is most significant at A1, and the acceleration peak values of these two sand fields at A3 after liquefaction are similar.

The Fourier transformation of the white noise signal at A1 is shown in Fig.12. The principal frequencies of both sand fields are 10 Hz before stimulating by the sinusoidal wave. The initial conditions of these two sand fields are close. Though no obvious attenuation occurs in the model foundation principal frequency after 0.2g sinusoidal wave stimulation, the obvious attenuation of high frequency component appears and the amplification of low frequency component. Different levels of softening occur at these two sand fields. The stiffness of model foundation decreases. The frequency spectra of these two sand fields are similar because they are arranged in the same test box.

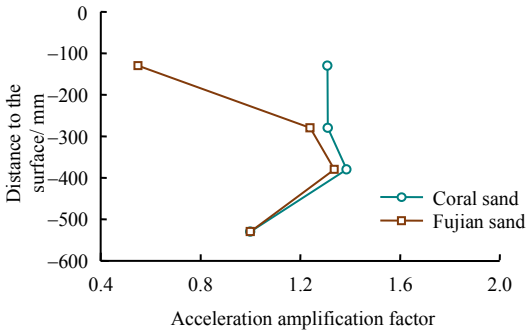

Fig.11 Acceleration amplification factors after liquefaction (a=0.2g)

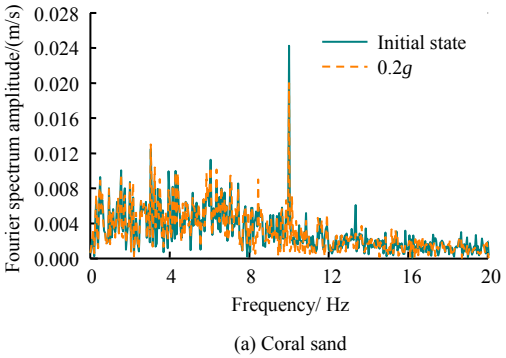

(a) Coral sand

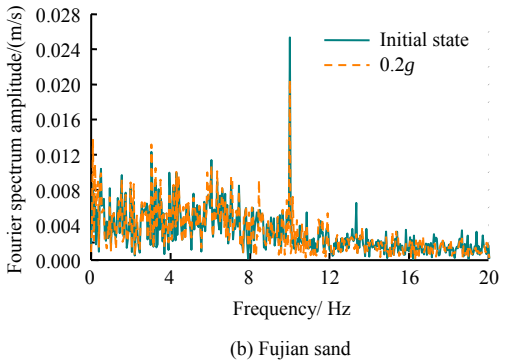

(b) Fujian sand

Fig.12 Acceleration Fourier spectra of two sand fields under different conditions

5 Analysis of building responses

Based on the fundamental theory of beam and mechanics of materials, the bending moment of building column and pile foundation is calculated as follows:

$$M = \frac{EI(\varepsilon_t - \varepsilon_c)}{h} \tag{2}$$

where ε_t and ε_c are the tensile and compressive strain, respectively; for the pile with square section, h is the square edge length; for the pile with circular section, h is the diameter; E and I are the elastic modulus and cross sectional moment of inertia.

The peak values of bending moment for building column and pile foundation are shown in Fig.13. In the working condition 1, the maximum bending moment for building column at the coral sand field is smaller than that of the Fujian sand field, with a ratio of 0.78–0.98. The maximum dynamical bending moment of building column at two sand fields occurs at the bottom section of columns in the ground floor, followed by the top and bottom sections of the second pile. It means that the dynamic bending moment of the medium standing column is larger, consisting with that of the dynamical bending moment response of the building column in earthquake conditions. The peak value of bending moment of pile foundation at the coral sand field is smaller than that of the Fujian sand field. The maximum dynamic bending moment of pile foundation at the two fields is at a 100 mm distance to the top of pile, followed

by the top of the pile. It is consistent with the phenomenon observed in the experiments of Suzuki et al.[19]. No liquefaction occurs at the sand fields and the inertia force is the main factor to affect the stress variation of pile foundation.

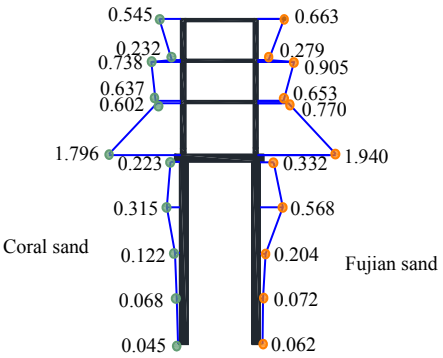

(a) Bending moment diagram at a=0.1g (unit: N • m)

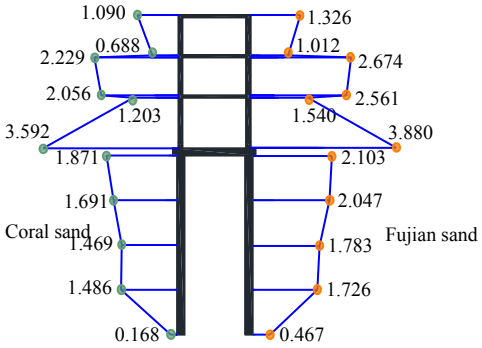

(b) Bending moment diagram at a=0.2g (unit: N • m)

Fig.13 Comparison of dynamic bending moment peak values for building column and pile foundation

For the working condition 2, the dynamic bending moment peak values of building column at the coral sand field are smaller than that of the Fujian sand field, i.e., with a ratio of 0.8–0.98. The variation rule of dynamic bending moment peak values of building column with depth is the same with that in the working condition 1. The bending moment peak values of pile foundation at the coral sand field are also smaller than that of the Fujian sand field. The maximum dynamic bending moment of pile foundation at two sand fields occurs at the top of pile. With depth, the bending moment peak values gradually decrease. Liquefied flow deformation occurs in the foundation soil. Deformation of sand soil is the main reason in affecting the internal force of pile foundation[29].

No liquefaction occurs in the coral sand field in the working condition 1 (0.1g). However, the bending moment of building column and pile foundation in the coral sand field of working condition 2 is about 2.0–3.2, and 3.7–21.8 times than that of the working condition 1. The bending moment of building column and pile foundation in the working condition 2 rapidly nonlinearly increases due to the liquefaction of coral sand field under the large acceleration condition. The soil is close to the liquid state without the shear strength. The decrease in stiffness results in the decrease in bonding effect of pile foundation. Compared with the non-liquid state, a much stronger shaking occurs in the building. The bending moment of building column rapidly increases, and the liquefied soil flows and forms an additional stress on the pile foundation. Thus, the bending moment of pile foundation increases. The amplification effect of building column and pile foundation at the Fujian sand field is similar with that of the coral sand field.

The horizontal displacement time history curves of building at the coral sand field and Fujian sand field are shown in Fig. 14. It demonstrates that the shaking amplitude of buildings at two sand fields increases with the input intensities in about 0–1.5 s. After the stabilization of input shaking intensities, the building shaking amplitude of two sand fields also keeps stable. At the end of the shaking test, the horizontal displacement of buildings at the coral sand field equals to about 0.27 times that of the Fujian sand field. For the working condition 2 (0.2g), the shaking amplitude of buildings at two sand fields increases rapidly at first. It begins to decrease after the peak value at 1.7 s when liquefaction state occurs at these two sand fields. The laser displacement sensors lose the target spot at the Fujian sand field at about 5.3 s due to the large subsidence of building at the Fujian sand field. The horizontal displacement of building at the coral sand field is larger than that of the Fujian sand field before 5.3 s. After the shaking test, the inclination of buildings along the vibration direction at these two sand fields is measured in Table 4. It is found that the inclination of buildings at the coral sand field is small. The inclination of buildings at the Fujian sand field is stronger than that of the coral sand field, presenting a consistent phenomenon with the dynamic triaxial tests observed in Sandoval et al.[8].

It shows that the linear subsidence of the building occurs during the shaking process at the coral sand field in the working conditions 1 and 2 in the Fig.15. The re-consolidation of soil induced by the dissipation of the excess pore pressure plays a minor role in the subsidence of buildings, which is consistent with the phenomenon observed in the experiments of terrigenous sand in Hausler[30]. A certain similarity of building subsidence exists in the coral sand and terrigenous sand. The subsidence characteristics of buildings at the Fujian sand field are the same with that of the coral sand. The building subsidence at the coral sand field in the working condition 2 rapidly increases and is about 49.3 times that in the working condition 1. After the input of 0.2g sine wave, liquefaction occurs at the coral sand field. The effective stress between the grains of foundation soil is close to 0, resulting in a decrease in the shear strength. A sharp decline of foundation bearing

capacity occurs and an obvious subsidence is found in the buildings. The binding effect of foundation soil on the pile foundation decreases, resulting in a sharp increase in the inclination of buildings in the working condition 2, i.e., 57.4 times that of the working condition 1. Compared with the working condition 1, the subsidence and inclination of buildings at the Fujian sand field obviously increase in the working condition 2.

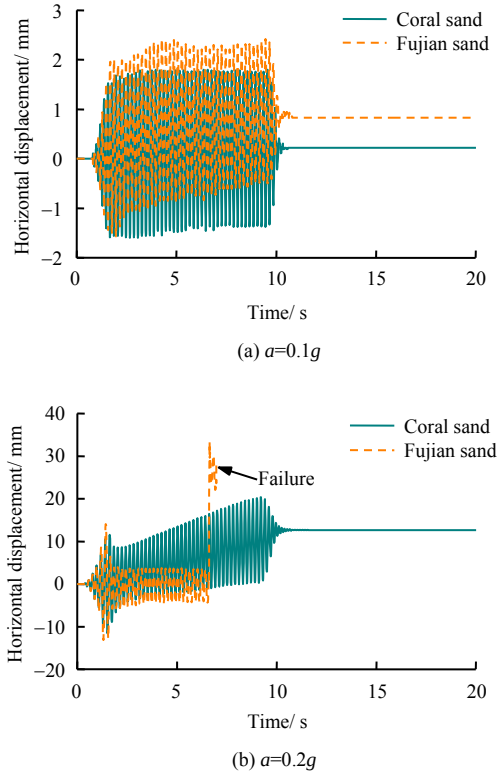

(a) a=0.1g

(b) a=0.2g

Fig.14 Time histories of horizontal displacement of model building

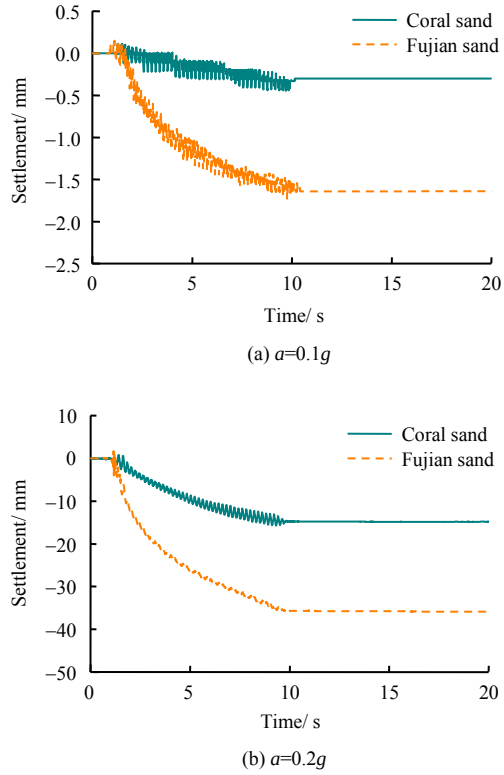

(a) a=0.1g

(b) a=0.2g

Fig.15 Time histories of model building settlement

Table 4 Displacement response of site under condition No.2

Types of fields	Angle of inclination/ (°)	Building subsidence/ mm	Surface subsidence / mm
Coral sand	2.4	14.8	1.1
Fujian sand	5.8	35.8	4.9

6 Conclusions

In order to study the dynamic response of foundation soil and building at the coral sand field and Fujian sand field under different earthquake intensities, parameters such as pore pressure, acceleration, dynamic bending moment, horizontal and vertical displacement, are measured based on shaking table tests. Some conclusions can be drawn as follows:

(1) The excess pore pressure ratio at two kinds of sand model foundation is far less than 1 under the stimulation of 0.1g sine wave. No liquefaction occurs in the model foundation. The excess pore pressure ratio at the coral sand field is about 0.5–0.6 of the Fujian sand field.

(2) After the stimulation input of 0.2g sine wave, the excess pore pressure at the coral sand is about 0.5–0.6 of the Fujian sand field. Under the same condition, the liquefaction of coral sand field is much difficult than that of the Fujian sand field.

(3) After the stimulation of 0.2g since wave, the amplification coefficient of acceleration peak at the coral sand field is about 1.1–2.4 times that of the Fujian sand field after liquefaction. Compared with the Fujian sand field, the model foundation of the liquefied coral sand field still has a certain stiffness and shear transfer capacity.

(4) Under different vibration intensities, the dynamic bending moments of the building column and pile foundation at the coral sand field are smaller than those of the Fujian sand field. The location of pile foundation for peak dynamic bending moment is different under the 0.1g and 0.2g vibration stimulation.

(5) Under the stimulation of sine wave of 0.1g and 0.2g, the final subsidence of buildings at the coral sand field is smaller than that of the Fujian sand field. The ratio of building subsidence at the coral sand field and the Fujian sand field is about 0.18 under the stimulation of 0.1g sine wave. The ratio changes to be 0.41 under the stimulation of 0.2g sine wave. The horizontal displacement of buildings at the coral sand field is also smaller than that of the Fujian sand field.

References

[1] LIU Chong-quan. The theory of calcareous soils mechanics and its application in engineering[D]. Wuhan: Institule of Rock and Soil Mechanics, Chinese Academy of Sciences, 1999.

[2] LIU Chong-quan, WANG Ren. Preliminary study on physical and mechanical properties of calcareous sand[J]. Rock and Soil Mechanics, 1998, 19(1): 32–37, 44.

[3] ZHU Chang-qi, CHEN Hai-yang, MENG Qing-shan, et al. Microscopic characterization of intra-pore structures of calcareous sands[J]. Rock and Soil Mechanics, 2014, 33(7): 1831–1836.

[4] HUANG Hong-xiang, CHEN Yu-min, WANG Jian-ping, et al. Ring shear tests on shear strength of calcareous sand[J]. Chinese Journal of Geotechnical Engineering, 2018, 39(6): 2082–2088.

[5] REN Yu-bin, WANG Yin, YANG Qing. Effects of particle size distribution and shape on permeability of calcareous sand[J]. Rock and Soil Mechanics, 2018, 39(2): 491–497.

[6] LIU Han-long, HU Ding, XIAO Yang, et al. Test study on dynamic liquefaction characteristics of calcareous sand[J]. Journal of Disaster Prevention and Mitigation Engineering, 2015, 35(6): 707–711.

[7] LIU Han-long, XIAO Peng, XIAO Yang, et al. Dynamic behaviors of MICP-treated calcareous sand in cyclic tests[J]. Chinese Journal of Geotechnical Engineering, 2018, 40(1): 38–45.

[8] SANDOVAL, PANDO E A, MIGUEL A. Experimental assessment of the liquefaction resistance of calcareous biogenous sands[J]. Earth Sciences Research Journal, 2012, 16(16): 55–63.

[9] SALEM M, ELMAMLOUK H, AGAIBY S. Static and cyclic behavior of north coast calcareous sand in Egypt[J]. Soil Dynamics and Earthquake Engineering, 2013, 55: 83–91.

[10] CARRARO J A H, BORTOLOTTO M S. Stiffness degradation and damping of carbonate and silica sands[M]//Frontiers in Offshore Geotechnics III. London: Taylor and Francis Group, 2015: 1179–1183.

[11] ANGEMEER J, CARLSON E D, STROUD S, et al. Pile load tests in calcareous soils conducted in 400 feet of water from a semi-submersible exploration rig[C]// Offshore Technology Conference. [S. l.]: [s. n.], 1975: 657–670.

[12] HASSANLOURAD M, SALEHZADEH H, SHAHNA-ZARIH. Strength of chemically grouted micro pile model in calcareous sand[C]//17th International Conference on Soil Mechanics and Geotechnical Engineering. Alexandria, Egypt: IOS Press, 2009.

[13] QIN Yue, MENG Qing-shan, WANG Ren, et al. A study on bearing characteristics of single pile in calcareous sand based on model experiment[J]. Rock and Soil Mechanics, 2015, 36(6): 1714–1720.

[14] JIANG Hao, WANG Ren, LÜ Ying-hui, et al. Test study of model pile in calcareous sands[J]. Rock and Soil Mechanics, 2010, 31(3): 780–784.

[15] CHAU K T, SHEN C Y, GUO X. Nonlinear seismic soil-pile-structure interactions: shaking table tests and FEM analyses[J]. Soil Dynamics and Earthquake Engineering, 2009, 29(2): 300–310.

[16] RASOULI R, TOWHATA I, HAYASHIDA T. Mitigation of seismic settlement of light surface structures by installation of sheet-pile walls around the foundation[J]. Soil Dynamics and Earthquake Engineering, 2015, 72: 108–118.

[17] TANG Liang, LING Xian-zhang, XU Peng-ju, et al. Shaking table test on seismic response of pile groups of bridges in liquefiable ground[J]. Chinese Journal of Geotechnical Engineering, 2010, 32(5): 672–680.

[18] CHEN Yue-qing. Shaking table test on dynamic interaction system of structure and foundation[D]. Shanghai: Tongji University, 2001.

[19] SUZUKI H, TOKIMATSU K, TABATA K. Factors affecting stress distribution of a 3×3 pile group in dry sand based on three-dimensional large shaking table tests[J]. Soils and Foundations, 2014, 54(4): 699–712.

[20] ZHANG Z, WEI H, QIN X. Experimental study on damping characteristics of soil-structure interaction system based on shaking table test[J]. Soil Dynamics and Earthquake Engineering, 2017, 98: 183–190.

[21] LU X, LI P, CHEN B, et al. Computer simulation of the dynamic layered soil pile structure interaction system[J]. Canadian Geotechnical Journal, 2005, 42(3): 742–751.

[22] SHAO Yi-fan, LAI Zheng-cong, PAN Wen, et al. Simplified method of isolation layer in shaking table test considered three-dimensional seismic effect[J]. Journal of Civil Architectural and Environmental Engineering, 2017, 39(2): 65–74.

[23] ZHANG Min-zheng. Study of similitude laws for shaking table tests[J]. Earthquake Engineering and Engi- neering Vibration, 1997, 17(2): 52–58.

[24] SUSUMU I. Similitude for shaking table test on soil-structure-fluid model 1*g* gravitational field[R]. Yokosuka: The Port and Harbour Reasearch Institute, Ministry of Transport, 1988.

[25] MA Xian-Feng, KONG Ling-gang, FANG Wei, et al. Parallel tests on preparation of samples with sand pourer[J]. Chinese Journal of Geotechnical Engi- neering, 2014, 36(10): 1791–1801.

[26] ZHUANG Hai-yang, YU Xu, ZHU Chao, et al. Shaking table tests for the seismic response of a base-isolated structure with the SSI effect[J]. Soil Dynamics and Earthquake Engineering, 2014, 67: 208–218.

[27] ZHANG Zhi-ying, WEI Hong-yang, QIN Xin. Experimental study on damping characteristics of soil-structure interaction system based on shaking table test[J]. Soil Dynamics and Earthquake Engineering, 2017, 98: 183–190.

[28] CHEN Yue-qing. Shaking table test on dynamic interaction system of structure and foundation[D]. Shanghai: Tongji University, 2001.

[29] YUAN Xiao-ming, LI Yu-run, SUN Rui. Mechanism of pile foundation response in liquefiable soils under seismic cyclic ground motion[J]. China Civil Engineering Journal, 2008, 41(9): 103–110.

[30] HAUSLER E A. Influence of ground improvement on settlement and liquefaction: a study based on field case history evidence and dynamic geotechnical centrifuge tests[D]. Berkeley: University of California, 2002.